Porous Coordination Polymers

DOI: 10.1002/ange.201300057

Mixed-Linker Hybrid Superpolyhedra for the Production of a Series of Large-Pore Iron(III) Carboxylate Metal–Organic Frameworks**

Hubert Chevreau, Thomas Devic, Fabrice Salles, Guillaume Maurin, Norbert Stock, and Christian Serre**

Metal–organic frameworks (MOFs) or porous coordination polymers (PCPs) with unprecedented diversity in terms of composition and structure have emerged over the years. They have attracted attention owing to their properties for several strategic applications, such as gas storage, separation, catalysis, energy storage, and more recently, biomedicine.[1] MOFs are formed through the iono–covalent association of inorganic moieties and organic molecules bearing complexing functionalities (e.g. carboxylates, azolates); often a 3D porous network results. So far, most MOFs are based on divalent cations (e.g. Zn^{2+}, Cu^{2+}, Ni^{2+}). Recent studies have shown that for a given carboxylate linker, the chemical stability, for example, towards hydrolysis, is improved when trivalent cations are used instead. However, the list of existing porous M^{3+}-based MOFs (e.g. with Al^{3+}, Fe^{3+}, Cr^{3+}, In^{3+}, V^{3+}, Sc^{3+}, Ln^{3+}) is still short,[2–6] and structures based on M^{4+} cations, such as Ti^{4+} or Zr^{4+}, are even more scarce.[7,8]

Among the possible trivalent metals, iron(III) is a highly promising candidate owing to its low toxicity, natural abundance, and redox properties. In the presence of carboxylates, iron(III) often leads to the formation of specific building units, such as isolated octahedra,[9] corner-sharing chains of octahedra,[10] helical chains,[11] oxo-centered trimers of octahedra (Figure 1 a),[5,12–14] and sometimes tetramers of octahedra.[15] In the case of oxo-centered trimers, the highly flexible MIL-88 solids are nice examples of tunable MOFs (MIL refers to a family of structures named as "Materials of Institut Lavoisier"). These structures contain spacers of different lengths and various functional groups; however, they have limitations in terms of their sorption properties owing to the contraction of their pores upon drying.[13] Particular attention has also been given to mesoporous iron-trimer-based di- or tricarboxylates, such as MIL-100(Fe),[5] MIL-101(Fe),[16] and more recently, PCN-53.[17] All of these solids are built up from hybrid superpolyhedra (supertetrahedra (STs) and superoctahedra (SOs) for MIL-100/101[4,18] and PCN-53, respectively), in which the vertices are occupied by iron(III/II) trimers, and polycarboxylate linkers lie at the edges or faces of the superpolyhedra. In the case of MIL-100 and MIL-101, the STs define extended hybrid analogues of the MTN zeolite structure (MTN = ZSM-39). Such solids exhibit mesoporous cages, which lead to very high specific Brunauer–Emmett–Teller (BET) surface areas above 2000 $m^2 g^{-1}$ and large pore volumes.

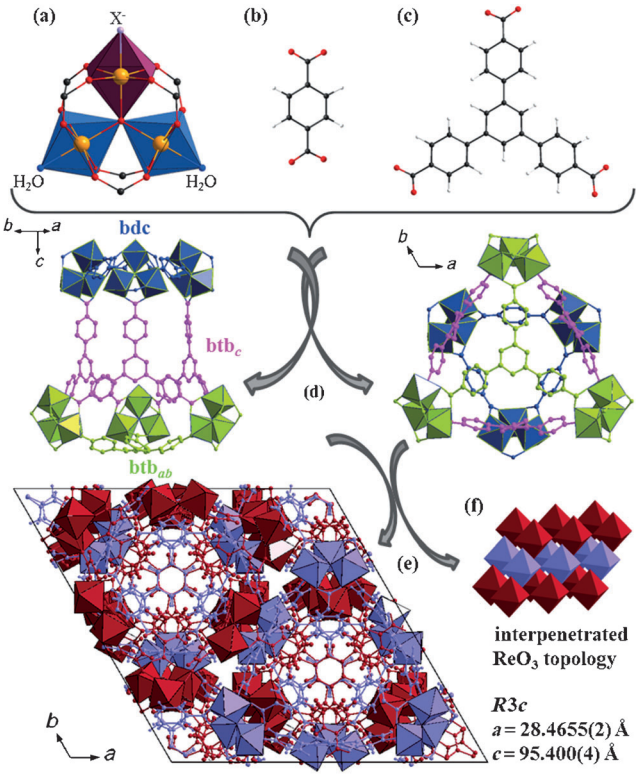

Figure 1. a) Oxo-centered trimer of FeO_6 octahedra in MIL-142A (Fe atoms: orange, O atoms: red, water molecules: blue, counteranion: purple); b) terephthalate (bdc); c) 1,3,5-benzenetrisbenzoate (btb); d) views of the hybrid superoctahedra along the *b* (left) and *c* axis (right); e) view of the structure of MIL-142 along the *c* axis; f) schematic representation of the interpenetrated ReO_3 topology.

[*] H. Chevreau, Dr. T. Devic, Dr. C. Serre
Institut Lavoisier (UMR CNRS 8180)
Université de Versailles Saint-Quentin-en-Yvelines
45 avenue des Etats-Unis, 78035 Versailles cedex (France)
E-mail: devic@chimie.uvsq.fr
serre@chimie.uvsq.fr
Dr. F. Salles, Prof. G. Maurin
Institut Charles Gerhardt Montpellier, Université Montpellier 2
Place E. Bataillon, 34095 Montpellier cedex 05 (France)
Prof. Dr. N. Stock
Institut für Anorganische Chemie, Christian-Albrechts-Universität
Max-Eyth-Strasse 2, 24118 Kiel (Germany)

[**] This research was supported by the European Commission through the FP7 European Project MACADEMIA (FP7/2007-2013) under grant agreement no. 228862. We thank Prof. Gérard Férey and Dr. Stuart Miller for fruitful discussions, the European Synchrotron Research Facilities (ESRF, Grenoble, France) for beam time, and Yaroslav Filinchuk and Herman Emerich of SNBL for technical support.

Supporting information for this article is available on the WWW under http://dx.doi.org/10.1002/anie.201300057.

Despite the existence of these structures, it is still a challenge to develop new porous iron(III)-based MOFs, which are of great interest for biomedicine,[19] catalysis,[5,20] and separation.[21] In the development of such MOFs, one has to face the difficulties related to the high chemical reactivity of iron(III). In solution, iron(III) either favors the formation of oxides/hydroxides, particularly when the temperature or the pH value is increased, or complicates the necessary control of the nucleation/growth process for the formation of suitable single crystals, a crucial prerequisite for structure determination.

One strategy for the development of new porous MOFs involves the use of a mixture of two ligands. This approach was successfully applied to the discovery of series of porous M^{2+}-based MOFs. The most significant examples, based on zinc or copper, are the microporous DMOFs (related to the original DMOF structure $[Zn(bdc)(dabco)_{0.5}]$ with a carboxylate ligand (bdc = 1,4-benzenedicarboxylic acid) and a diamine ligand (dabco = 1,4-diazabicyclo[2.2.2]octane)),[22] mesoporous DUT-6 (named after the Dresden University of Technology),[26] UMCMs (named as "University of Michigan Crystalline Materials",[24,25] MOF-205,[12] and MOF-210 (with dicarboxylate and tricarboxylate ligands).[26]

We followed this approach and focused our attention on the reactivity of Fe^{III} cations in the presence of mixtures of 1,4-benzenedicarboxylic acid (terephthalic acid or H_2bdc; Figure 1b) and 1,3,5-tris(4-carboxyphenyl)benzene (1,3,5-benzenetrisbenzoic acid or H_3btb; Figure 1c). We used a high-throughput solvothermal synthesis methodology[27] and isolated two new porous crystalline MOFs: MIL-142A, a microporous interpenetrated structure, and MIL-143, a mesoporous zeotypic solid.

The structure of MIL-142A was solved by single-crystal diffraction with synchrotron radiation (ESRF, Grenoble, France). MIL-142A or $[Fe_3O(H_2O)_2(Cl^-)(bdc)(btb)_{4/3}]\cdot n$solv exhibits a microporous interpenetrated rhombohedral structure (*R*3*c* (no. 161), $a = 28.4655(2)$, $c = 95.400(4)$, $V = 66\,944.7(6)$ Å^3; Figure 1), which consists of iron(III) trimers of FeO_6 octahedra (Figure 1a) interconnected by two bdc and four btb ligands to form distorted hybrid superoctahedra (Figure 1d), in which the btb ligands occupy four faces (one (btb_{ab}) lies in the *ab* plane and three (btb_c) are parallel to the *c* axis), and the bdc ligands occupy the remaining three edges. To the best of our knowledge, these hybrid units have not been observed previously. They can be described as a merging of the ST from MIL-101 and the extended ST of MIL-100, in which the trimesate ligand (btc) is replaced with btb. An extended ST of the latter type has been observed previously within a porous Sc–btb MOF.[6] The replacement of a trimer from one vertix of the extended MIL-100 ST with one face of the MIL-101 ST, which consists of three trimers linked by three bdc ligands, leads to the SO of MIL-142A (see Figure S1 in the Supporting Information). SOs are then connected at their corners through the trimers to give a ReO_3-type net with cubic–octahedral mesoporous interstices. These interstices contain the SOs of a second ReO_3 net, which leads to the interpenetrated structure (Figure 1e,f). The resulting short distances between π-stacked btb ligands ($d_{C\cdots C} = 3.60$ and 3.86 Å for btb_{ab} and btb_c, respectively) may indicate the presence of inter-network π–π interactions.[24] These short distances result in a rigid structure with tunnels running along the *a* and *b* axes ($\phi \approx 7$ Å). The thermal stability in air of MIL-142A is close to 250 °C, as shown by thermogravimetric analysis and temperature-dependent X-ray powder diffraction (see Figures S10–S14). The nitrogen-sorption isotherm at 77 K is of type I, in agreement with the microporous character of MIL-142A, and leads to a BET surface area of 1580(20) $m^2 g^{-1}$ (see Figure S23). This value is in agreement with the theoretical accessible surface area (ca. 1900 $m^2 g^{-1}$) calculated by using a geometrical method based on a Monte Carlo approach (see Table S3 and related discussion in the Supporting Information).[25] The free volume is close to 0.75 $cm^3 g^{-1}$, in agreement with the measured value (0.70 $cm^3 g^{-1}$).[30]

One strategy for the functionalization of the pores of MOFs involves the use of bdc derivatives bearing polar or apolar groups.[3,13,26,31] 2-Aminoterephthalic (bdc-NH_2) and 2-nitroterephthalic acid (bdc-NO_2) were used to produce MIL-142A_NH_2 and MIL-142A_NO_2, respectively (see the Supporting Information for more details). The resulting BET surface areas and pore volumes (1390(20) $m^2 g^{-1}$, 0.69 $cm^3 g^{-1}$ and 1340(20) $m^2 g^{-1}$, 0.69 $cm^3 g^{-1}$ for the NH_2 and NO_2 derivatives, respectively) are, as expected, slightly lower than those in the pristine material, but are in fair agreement with the theoretical values (1660 $m^2 g^{-1}$, 0.70 $cm^3 g^{-1}$ and 1600 $m^2 g^{-1}$, 0.68 $cm^3 g^{-1}$, respectively). It is also well-documented that isoreticular series of MOFs can be obtained with dicarboxylate linkers, whereby the use of longer linkers leads to an increase in the pore size and surface area.[32] To our knowledge, such a strategy has been applied only to the DMOF[22] and UMCM[24,25] series of mixed-carboxylate systems.

Remarkably, one can produce larger analogues of MIL-142A by using 2,6-naphthalenedicarboxylate (2,6-ndc: MIL-142B), 4,4′-biphenyldicarboxylate (bpdc: MIL-142C), 1,4-phenylenediacrylate (pdac: MIL-142D), or 4,4′-azobenzenedicarboxylate (azodc: MIL-142E). The unit cells of these structures were determined by powder X-ray diffraction (see the Supporting Information). An increase in the length of the linkers resulted in an increase in the unit-cell volume from 66 944(1) (MIL-142A) up to 95 547(3) Å^3 (MIL-142E). The higher volumes are associated with a significant increase in the *a* parameter, from 28.4655(2) Å in MIL-142A to 34.5966(7) Å in MIL-142E, but a small decrease in the *c* parameter, from 95.400(4) Å to 92.176(2) Å (Figure 2; see also the Supporting Information). An analysis of the SO can readily explain this phenomenon: the three trimers located at the top of the SO shown in Figure 1d are connected to each other through three dicarboxylate ligands (in blue), whereas the three trimers at the bottom are linked by one btb_{ab} ligand only (in green); all of these ligands lie in the *ab* plane. These trimers are then connected along the *c* axis through three different btb_c ligands (in pink). When the length of the linear linker increases, the distances between the trimers in the *ab* plane at the top of the SO increase, whereas those between the trimers at the bottom remain constant. As a result, the *a* parameter increases (as does the *b* parameter), which forces the btb_c ligands to adopt an orientation that is no longer

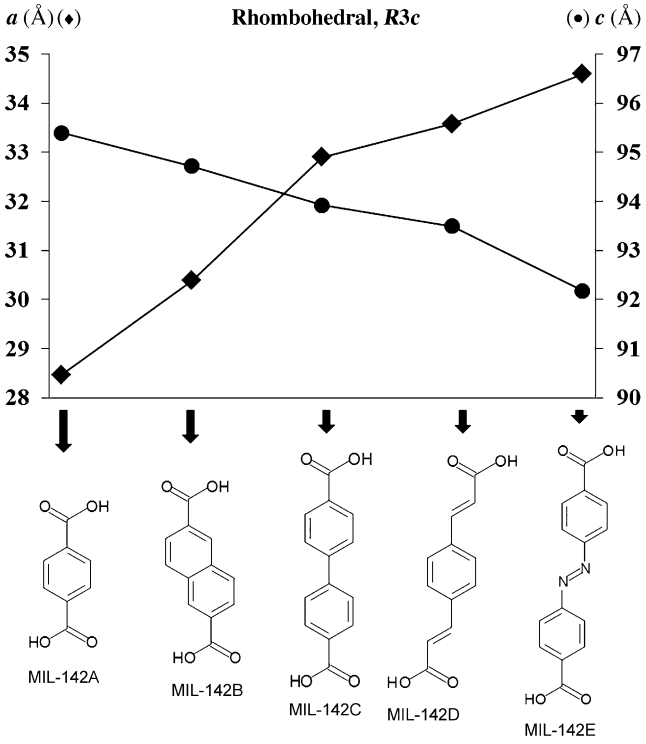

Figure 2. Experimental unit-cell parameters of MIL-142 as a function of the dicarboxylate linker (see the Supporting Information for more details).

parallel to the *c* axis and thus induces the slight decrease in the *c* parameter (Figure 1 d). We used the experimental cell parameters to simulate the crystal structures of this isoreticular series by using a ligand-replacement computational strategy (see the Supporting Information).[3,13,27,33] This approach enabled the estimation of the theoretical accessible surface areas and free volumes of the solids MIL-142B–E (see Table S3). As expected, both the accessible surface area and the pore volume increase with the length of the linker. They reach approximately 2800 $m^2 g^{-1}$ and 1.1 $cm^3 g^{-1}$, respectively, for MIL-142E. In the same way, the pore diameter increases from 8 in MIL-142A to 12.2 Å in MIL-142E (see Table S1). A second consequence of the pore expansion is the formation of very narrow tunnels along the *c* axis with coordinated water molecules from the iron(III) trimers along their surfaces. Although not accessible in their hydrated form ($\phi \approx 0.7$–2.8 Å), these tunnels might become accessible in their dehydrated form, as most MOFs based on iron(III) trimers are stable upon the departure of bound water.[20]

Besides the feasibility of mixed-ligand iron(III) carboxylate MOFs, increasing the pore size is still a great challenge, particularly for larger-pore structures, which are of a great interest for the controlled release of very large bioactive molecules.[19] Extending the length of the polycarboxylate ligands is a known successful strategy for building up mesoporous materials, particularly with the very large btb ligand.[19,24,25] However, as for the MIL-142 series of solids, the risk is high that ligand extension may be associated with interpenetration of the framework.[29]

During our study on the ex situ crystallization of MIL-142A, we observed that although long reaction times (> 25 h) led to pure MIL-142A, in the initial stage of the reaction, another crystalline phase was formed. The structure of this compound, denoted MIL-143, was solved from X-ray powder diffraction synchrotron data (beamline BM01A, ESRF, Grenoble, France; see the Supporting Information for details). MIL-143 or $[Fe_3O(Cl^-)(H_2O)_2(bdc)_{3/2}(btb)]\cdot n$solv crystallizes in the cubic *F*23 (no. 196) space group ($a =$ 40.8635(1) Å).

Oxo-centered trimers of iron(III) octahedra constitute the primary building unit. They assemble with the ligands to give two types of ST: the first is similar to those of MIL-100, but with btb instead of btc on the faces, and the second is identical to those of MIL-101, that is, with bdc on the edges. Indeed, the structure of MIL-143 can be considered as a succession of extended STs of MIL-100 and STs of MIL-101 (Figure 3 a).

The unit cell is thus built up from a central extended MIL-100 ST connected to four MIL-101 STs (Figure 3 c). In a similar way to the construction of MIL-100 and MIL-101, this arrangement leads to the formation of two sets of mesoporous cages with free diameters of 20 and 24 Å. The larger cage, capped by four faces of MIL-101 STs and six edges of extended MIL-100 STs, are accessible through windows of approximately 16 Å. The smaller cage, delimited by four faces of extended MIL-100 STs and six edges of extended MIL-100 STs, are accessible through windows with a free diameter of 18 Å (Figure 3 b,b′).

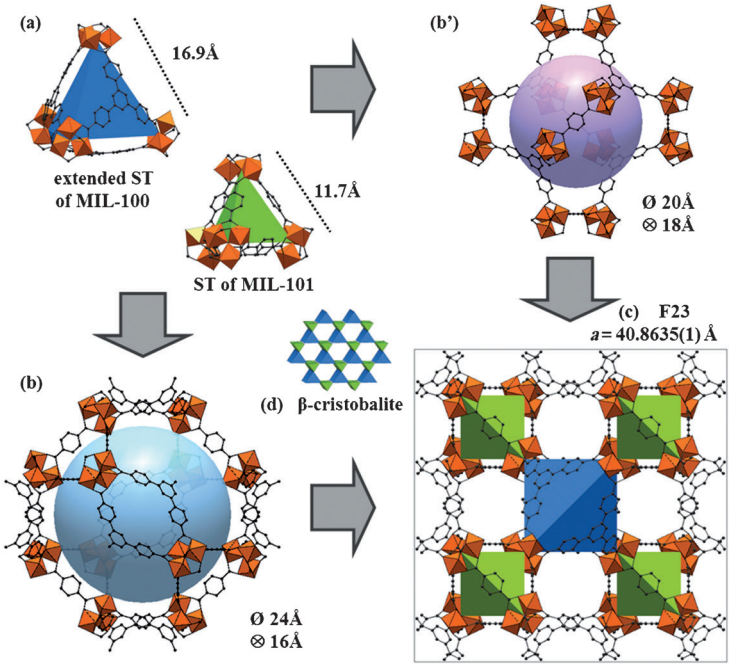

Figure 3. a) Extended supertetrahedra of MIL-100 and supertetrahedra of MIL-101; b,b′) mesoporous cages of MIL-143; c) view of the structure; d) schematic representation of the β-cristobalite topology.

In contrast to MIL-100 and MIL-101, which both exhibit a zeotypic MTN architecture, MIL-143 is a rare example of an extended hybrid form of the β-cristobalite structure (Figure 3d). Thermogravimetric analysis and temperature-dependent X-ray powder diffraction indicate a thermal stability of approximately 200 °C in air (see Figures S12 and S14). As expected, nitrogen adsorption shows a type IV isotherm, with a substep at $P/P_0 = 0.09$, characteristic of a mesoporous solid. The resulting experimental pore volume and accessible surface area reached 1.18 $cm^3 g^{-1}$ and 2150 $m^2 g^{-1}$, respectively (see Figure S25), which are lower than the theoretical values extracted from the crystal structure (2.15 $cm^3 g^{-1}$ and 3540 $m^2 g^{-1}$, respectively). This difference is probably due to the partial activation of the solid; all attempts to improve the activation, including the use of supercritical CO_2, were unsuccessful, probably owing to poisoning by impurities at the Lewis acidic metal sites. Like MIL-142A, MIL-143 can also be functionalized with the bdc ligand, for example, by the use of bdc-NH_2, which led to a pore volume of 1.10 $cm^3 g^{-1}$ and a BET surface area above 2100 $m^2 g^{-1}$ (theoretical values: 2.08 $cm^3 g^{-1}$ and 3480 $m^2 g^{-1}$, respectively; see Table S3). The removal of impurities, such iron oxide, the ligand, and *N*,*N*-dimethylformamide, can be challenging, particularly from fragile MOFs, and our efforts to purify MIL-143 were unsuccessful (see Figures S12 and S22).[30]

MIL-142 and MIL-143 are both built up from trimers of iron octahedra and contain dicarboxylate linkers that can be functionalized readily. To our knowledge, MOFs that combine permanent porosity, Lewis acidity, and organic functionalization are rather rare. For example, the highly flexible MIL-88 series based on FeO_6 trimers possess two types of groups but suffer from the absence of significant porosity for light gases owing to their significant contraction upon drying.[5] Thus, as it was shown previously that both Lewis acidity and polar organic groups (e.g. NO_2, NH_2) could enhance the separation abilities of MOFs for various gaseous mixtures, the MIL-142 and MIL-143 series can be considered as promising candidates for separation-related applications.

In conclusion, a series of new micro-/mesoporous MOFs based on iron(III) trimers of octahedra and mixtures of di- and tricarboxylate linkers have been isolated and their structures solved from a combination of X-ray diffraction data and computational tools. The first series, MIL-142, presents an interwoven structure whose 2D microporous system can be tuned in size and shape and/or functionalized through the use a variety of dicarboxylate linkers. MIL-143 is the first example of an iron(III) mesoporous MOF based on different hybrid supertetrahedra and exhibits a rare extended β-cristobalite structure.

Experimental Section

The Supporting Information contains the synthetic procedures for the preparation of the MIL-142 series and MIL-143, together with details on the crystal-structure determination of MIL-142A and MIL-143 and on the simulation-assisted structure determination of MIL-142B, MIL-142C, MIL-142D, and MIL-142E. Elemental analysis, thermogravimetric analysis, temperature-dependent X-ray powder diffraction, infrared spectroscopy, and nitrogen-sorption measurements are also described.

Received: January 4, 2013
Published online: April 3, 2013

Keywords: carboxylate ligands · iron · mesoporous materials · metal–organic frameworks · microporous materials

[1] *Chem. Soc. Rev.* **2009**, *38*, 1203; *Chem. Rev.* **2012**, *112*, 673.
[2] T. Ahnfeldt, N. Guillou, D. Gunzelmann, I. Margiolaki, T. Loiseau, G. Férey, J. Senker, N. Stock, *Angew. Chem.* **2009**, *121*, 5265; A. Lieb, H. Leclerc, T. Devic, C. Serre, I. Margiolaki, F. Mahjoubi, J. S. Lee, A. Vimont, M. Daturi, J.-S. Chang, *Microporous Mesoporous Mater.* **2012**, *157*, 18; Y. L. Liu, J. F. Eubank, A. J. Cairns, J. Eckert, V. C. Kravtsov, R. Luebke, M. Eddaoudi, *Angew. Chem.* **2007**, *119*, 3342; *Angew. Chem. Int. Ed.* **2007**, *46*, 3278.
[3] T. Devic, P. Horcajada, C. Serre, F. Salles, G. Maurin, B. Moulin, D. Heurtaux, G. Clet, A. Vimont, J.-M. Grenèche, B. L. Ouay, F. Moreau, E. Magnier, Y. Filinchuk, J. Marrot, J.-C. Lavalley, M. Daturi, G. Férey, *J. Am. Chem. Soc.* **2010**, *132*, 1127.
[4] G. Férey, C. Mellot-Draznieks, C. Serre, F. Millange, J. Dutour, S. Surblé, I. Margiolaki, *Science* **2005**, *309*, 2040.
[5] P. Horcajada, S. Surblé, C. Serre, D.-Y. Hong, Y.-K. Seo, J.-S. Chang, J.-M. Grenèche, I. Margiolaki, G. Férey, *Chem. Commun.* **2007**, 2820.
[6] I. A. Ibarra, X. Lin, S. Yang, A. J. Blake, G. S. Walker, S. A. Barnett, D. R. Allan, N. R. Champness, P. Hubberstey, M. Schröder, *Chem. Eur. J.* **2010**, *16*, 13671.
[7] M. Dan-Hardi, C. Serre, T. Frot, L. Rozes, G. Maurin, C. Sanchez, G. Férey, *J. Am. Chem. Soc.* **2009**, *131*, 10857; Y. Fu, D. Sun, Y. Chen, R. Huang, Z. Ding, X. Fu, Z. Li, *Angew. Chem.* **2012**, *124*, 3420; *Angew. Chem. Int. Ed.* **2012**, *51*, 3364; C. Zlotea, D. Phanon, M. Mazaj, D. Heurtaux, V. Guillerm, C. Serre, P. Horcajada, T. Devic, E. Magnier, F. Cuevas, G. Férey, P. L. Llewellyn, M. Latroche, *Dalton Trans.* **2011**, *40*, 4879.
[8] V. Bon, V. Senkovskyy, I. Senkovska, S. Kaskel, *Chem. Commun.* **2012**, *48*, 8407; J. H. Cavka, S. Jakobsen, U. Olsbye, N. Guillou, C. Lamberti, S. Bordiga, K. P. Lillerud, *J. Am. Chem. Soc.* **2008**, *130*, 13850; K. E. deKrafft, W. S. Boyle, L. M. Burk, O. Z. Zhou, W. Lin, *J. Mater. Chem.* **2012**, *22*, 18139; V. Guillerm, S. Gross, C. Serre, T. Devic, M. Bauer, G. Férey, *Chem. Commun.* **2010**, *46*, 767; M. Lin Foo, S. Horike, T. Fukushima, Y. Hijikata, Y. Kubota, M. Takata, S. Kitagawa, *Dalton Trans.* **2012**, *41*, 13791; W. Morris, B. Volosskiy, S. Demir, F. Gándara, P. L. McGrier, H. Furukawa, D. Cascio, J. F. Stoddart, O. M. Yaghi, *Inorg. Chem.* **2012**, *51*, 6443.
[9] A. Fateeva, S. Devautour-Vinot, N. Heymans, T. Devic, J.-M. Grenèche, S. Wuttke, S. Miller, A. Lago, C. Serre, G. De Weireld, G. Maurin, A. Vimont, G. Férey, *Chem. Mater.* **2011**, *23*, 4641.
[10] A. Fateeva, P. Horcajada, T. Devic, C. Serre, J. Marrot, J.-M. Grenèche, M. Morcrette, J.-M. Tarascon, G. Maurin, G. Férey, *Eur. J. Inorg. Chem.* **2010**, 3789; F. Millange, C. Serre, N. Guillou, G. Férey, R. I. Walton, *Angew. Chem.* **2008**, *120*, 4168; *Angew. Chem. Int. Ed.* **2008**, *47*, 4100; T. R. Whitfield, X. Wang, L. Liu, A. J. Jacobson, *Solid State Sci.* **2005**, *7*, 1096.
[11] C. Serre, F. Millange, S. Surblé, J. M. Grenèche, G. Férey, *J. Am. Chem. Soc.* **2004**, *126*, 6.
[12] E. Haque, J. W. Jun, S. H. Jhung, *J. Hazard. Mater.* **2011**, *185*, 507.
[13] P. Horcajada, F. Salles, S. Wuttke, T. Devic, D. Heurtaux, G. Maurin, A. Vimont, M. Daturi, O. David, E. Magnier, N. Stock, Y. Filinchuk, D. Popov, C. Riekel, G. Férey, C. Serre, *J. Am. Chem. Soc.* **2011**, *133*, 17839.
[14] C. Serre, S. Surblé, C. Mellot-Draznieks, Y. Filinchuk, G. Férey, *Dalton Trans.* **2008**, 5462.
[15] S. B. Choi, M. J. Seo, M. Cho, Y. Kim, M. K. Jin, D.-Y. Jung, J.-S. Choi, W.-S. Ahn, J. L. C. Rowsell, J. Kim, *Cryst. Growth Des.* **2007**, *7*, 2290.

[16] D. Lupu, O. Ardelean, G. Blanita, G. Borodi, M. D. Lazar, A. R. Biris, C. Ioan, M. Mihet, I. Misan, G. Popeneciu, *Int. J. Hydrogen Energy* **2011**, *36*, 3586.
[17] D. Yuan, R. B. Getman, Z. Wei, R. Q. Snurr, H.-C. Zhou, *Chem. Commun.* **2012**, *48*, 3297.
[18] G. Férey, C. Serre, C. Mellot-Draznieks, F. Millange, S. Surblé, J. Dutour, I. Margiolaki, *Angew. Chem.* **2004**, *116*, 6456; *Angew. Chem. Int. Ed.* **2004**, *43*, 6296.
[19] P. Horcajada, T. Chalati, C. Serre, B. Gillet, C. Sebrie, T. Baati, J. F. Eubank, D. Heurtaux, P. Clayette, C. Kreuz, J.-S. Chang, Y. K. Hwang, V. Marsaud, P.-N. Bories, L. Cynober, S. Gil, G. Férey, P. Couvreur, R. Gref, *Nat. Mater.* **2010**, *9*, 172 – 178.
[20] A. Dhakshinamoorthy, M. Alvaro, H. Chevreau, P. Horcajada, E. Gibson, M. Vishnuvarthan, A. Vimont, J. M. Grenèche, M. Daturi, T. Devic, C. Serre, H. García, *ACS Catal. Sci. Tech.* **2012**, *2*, 3242060.
[21] M. Maes, M. Trekels, M. Boulhout, S. Schouteden, F. Vermoortele, L. Alaerts, D. Heurtaux, Y.-K. Seo, Y.-K. Hwang, J.-S. Chang, I. Beurroies, R. Denoyel, K. Temst, A. Vantomme, P. Horcajada, C. Serre, D.-E. De Vos, *Angew. Chem.* **2011**, *123*, 4296 – 4300; *Angew. Chem. Int. Ed.* **2011**, *50*, 4210 – 4214; E. D. Bloch, W. L. Queen, R. Krishna, J. M. Zadrozny, C. M. Brown, J. R. Long, *Science* **2012**, *335*, 1606 – 1610.
[22] D. N. Dybtsev, H. Chun, K. Kim, *Angew. Chem.* **2004**, *116*, 5143; *Angew. Chem. Int. Ed.* **2004**, *43*, 5033.
[23] N. Klein, I. Senkovska, K. Gedrich, U. Stoeck, A. Henschel, U. Mueller, S. Kaskel, *Angew. Chem.* **2009**, *121*, 10139; *Angew. Chem. Int. Ed.* **2009**, *48*, 9954.
[24] K. Koh, J. D. Van Oosterhout, S. Roy, A. G. Wong-Foy, A. J. Matzger, *Chem. Sci.* **2012**, *3*, 2429.
[25] K. Koh, A. Wong-Foy, A. Matzger, *Angew. Chem.* **2008**, *120*, 689; *Angew. Chem. Int. Ed.* **2008**, *47*, 677; K. Koh, A. G. Wong-Foy, A. J. Matzger, *J. Am. Chem. Soc.* **2010**, *132*, 15005; K. Koh, A. G. Wong-Foy, A. J. Matzger, *J. Am. Chem. Soc.* **2009**, *131*, 4184.
[26] H. Furukawa, N. Ko, Y. B. Go, N. Aratani, S. B. Choi, E. Choi, A. Ö. Yazaydin, R. Q. Snurr, M. O'Keeffe, J. Kim, O. M. Yaghi, *Science* **2010**, *329*, 424.
[27] N. Stock, *Microporous Mesoporous Mater.* **2010**, *129*, 287; N. Stock, S. Biswas, *Chem. Rev.* **2012**, *112*, 933.
[28] C. R. Martinez, B. L. Iverson, *Chem. Sci.* **2012**, *3*, 2191.
[29] T. Düren, F. Millange, G. Férey, K. S. Walton, R. Q. Snurr, *J. Phys. Chem. C* **2007**, *111*, 15350.
[30] H. Frost, T. Düren, R. Q. Snurr, *J. Phys. Chem. B* **2006**, *110*, 9565.
[31] H. Deng, C. J. Doonan, H. Furukawa, R. B. Ferreira, J. Towne, C. B. Knobler, B. Wang, O. M. Yaghi, *Science* **2010**, *327*, 846; S. Biswas, T. Ahnfeldt, N. Stock, *Inorg. Chem.* **2011**, *50*, 9518.
[32] M. Eddaoudi, J. Kim, N. Rosi, D. Vodak, J. Wachter, M. O'Keeffe, O. M. Yaghi, *Science* **2002**, *295*, 469; S. Surblé, C. Serre, C. Mellot-Draznieks, F. Millange, G. Férey, *Chem. Commun.* **2006**, 284.
[33] F. Salles, G. Maurin, C. Serre, P. L. Llewellyn, C. Knôfel, H. J. Choi, Y. Filinchuk, L. Oliviero, A. Vimont, J. R. Long, G. Férey, *J. Am. Chem. Soc.* **2010**, *132*, 13782.
[34] J. W. Yoon, Y.-K. Seo, Y. K. Hwang, J.-S. Chang, H. Leclerc, S. Wuttke, P. Bazin, A. Vimont, M. Daturi, E. Bloch, P. L. Llewellyn, C. Serre, P. Horcajada, J.-M. Grenèche, A. E. Rodrigues, G. Férey, *Angew. Chem.* **2010**, *122*, 6085; *Angew. Chem. Int. Ed.* **2010**, *49*, 5949.
[35] W. Xuan, C. Zhu, Y. Liu, Y. Cui, *Chem. Soc. Rev.* **2012**, *41*, 1677.

